Preformulation Characterization of Hydroxypropyl Cellulose Microparticles for Drug Delivery Applications: A Basis for Rational Design and Process Optimization

T. Georgievska,[a,*] S. Trajkovic,[b] D. Stojanov,[b] M. Stojanovska Pecova,[b] and K. Lisichkov[c]

[a]Quality Assurance, Alkaloid AD Skopje, Bul. Aleksandar Makedonski 12, R. of North Macedonia

[b]Research and Development, Alkaloid AD Skopje, Bul. Aleksandar Makedonski 12, R. of North Macedonia

[c]Faculty of Technology and Metallurgy, Skopje, Ruđer Bošković 16, R. of North Macedonia

doi: https://doi.org/10.15255/CABEQ.2025.2443

Original scientific paper
Received: August 23, 2025
Accepted: November 4, 2025

This study explores early formulation parameters influencing hydroxypropyl cellulose (HPC)-based microparticles as carriers for paracetamol, with the aim of establishing a modified-release drug delivery system and informing future design optimization. Microparticles were prepared via the oil-in-oil emulsion/solvent evaporation method using acetone, HPC as a thermo-responsive polymer, and Tween 80 as a non-conventional surfactant. Polymer content and phase ratio were varied to assess effects on encapsulation efficiency and dissolution behavior. Characterization by FTIR, DSC, UV-Vis, laser diffraction, and microscopy confirmed spherical morphologies (495–760 μm), thermal stability, and successful drug encapsulation (up to 73 %). *In vitro* dissolution at pH 6.8 revealed modified release profiles, with kinetics best described by the Weibull model, indicating Fickian diffusion as the dominant mechanism. Polymer content emerged as the key variable affecting critical quality attributes. These findings provide a foundation for rational formulation and process optimization, to be further refined through D-optimal experimental design.

Key words

acetaminophen, oil-in-oil emulsion solvent evaporation method, drug delivery systems, hydroxypropyl cellulose

Introduction

Paracetamol is a weak cyclooxygenase (COX) enzyme inhibitor and is a common over-the-counter (OTC) analgesic and antipyretic that is usually administered for fever, temperature relief, or in long-term treatment of pain (e.g., arthritis). It has a relatively short elimination half-life, varying from about 1 to 3 hours. It is rapidly absorbed in the small intestine and quickly metabolized in the liver, followed by urine excretion as an inactive glucuronide and sulfate conjugates. Due to the high drug elimination (up to 98 %) after a single oral dose[1] the treatment requires frequent dosing to maintain the blood plasma concentration, and an acute overdose of paracetamol may potentially cause liver damage[2]. In therapeutic doses, paracetamol is a safe analgesic, but in overdosage, it can cause severe hepatic necrosis.

According to the Therapeutic Goods Administrations (TGA) of the Australian Government, the recommended regime for paracetamol dosing is 500 mg to 1000 mg every 4 to 6 hours as necessary, with a maximum daily dose (MDD) of 4000 mg for adults and children above 12 years[3]. Considering the international measurements and changes[4], and in order to minimize the risk of hepatotoxicity and overdosing due to self-poisoning, Australia's drug regulator announced that, effective 1 February 2025, paracetamol pack sizes and availability will be reduced. Similarly, the U.S. Food and Drug Administration (FDA) proposed lowering the MDD from 3900–4000 mg to 3000–3250 mg. In 2018, the European Medicines Agency (EMA) suspended modified- or prolonged-release paracetamol products from the EU market[5] due to difficulties in overdose management and the lack of scientifically substantiated data distinguishing overdoses caused by immediate-release or prolonged-release formulations—each requiring distinct treatment approaches[5]. These developments highlight the need for a new

*Corresponding author: tgeorgievska@alkaloid.com.mk

research field into sustained-release paracetamol formulations to reduce dosing frequency and minimize dose dumping. Sustained-release paracetamol formulations can potentially reduce dosing to three times a day[6].

Stimuli-responsive polymers or polymer blends have attracted significant research attention in recent decades. With the growing trend in eco-consumerism, environmental sustainability, green engineering and chemistry, and the circular economy, as well as vegetarian principles, recent research primarily focuses on cellulose-based polymers[7]. Hydroxypropyl methylcellulose (HPMC) has been utilized in the oil-in-oil (O/O) emulsion/solvent evaporation (ESE) method for encapsulating meloxicam[8], in the water-in-oil (W/O) ESE method for encapsulating fexofenadine HCl[9], and as an excipient[10] in the co-evaporation technique following the ESE process to encapsulate the model drug quercetin. Hydroxypropyl cellulose (HPC) has been used in spray-freeze-drying technology to encapsulate diterpenoid lactone[11]. It has been reported that HPC is mainly used as a carrier of solid dispersions of poorly soluble drugs (felodipine[12] and ezetimibe[13]). No studies have been reported on the use of HPC in the ESE method.

Hydroxypropyl cellulose is a nonionic cellulose ether biopolymer belonging to the polysaccharide class. It is used as an emulsifier in cosmetics, and as a flocculant, plasticizer, and binding agent in pharmaceutical formulations[14,15]. According to Ph. Eur. 0337 [16], HPC is defined as partially *O*-(2-hydroxypropylated) cellulose containing 53.4 % to 80.5 % hydroxypropyl groups (dried substance).

However, the practical application of HPC is limited by its lower critical solution temperature (LCST) of 40 –45 °C [17], which poses challenges for applications close to the physiological temperature range of 25–38 °C. Despite this, cellulose derivatives have become essential biocompatible materials in biomedical and pharmaceutical fields due to their favorable physical and mechanical characteristics, low toxicity, biocompatibility, and biodegradability[18]. Non-aqueous (O/O) emulsions, composed of two non-aqueous liquids, have been rarely used as an alternative system for microencapsulation of active pharmaceutical ingredients (API). In the literature[19], non-aqueous emulsions in pharmaceutical technology have been utilized for entrapping hydrolytically unstable drugs. Recent studies have reported the encapsulation of oxalic acid in acrylonitrile-butadiene-styrene *via* the O/O ESE method. To the best of our knowledge, no other studies have been identified in the existing literature that explore oil-in-oil (O/O) ESE methods for microencapsulation[20].

Sorbitan monooleate 80 (Span 80) with a hydrophilic-lipophilic balance (HLB) value of approximately 4.3 [21], is the most used stabilizer in non-aqueous emulsions. No studies have reported the use of polyoxyethylene-80-sorbitan monooleate (Tween 80) in O/O emulsions with an HLB of approximately 15 [21]. In the study[22], colloid-chemical aspects were investigated among aqueous solution of HPC and Tween 80. Synergistic effects were observed with respect to interfacial energy reduction, due to the formation of a Tween 80-HPC bilayer *via* hydrogen bonding between the hydroxyl groups from HPC and ethoxy units of Tween 80.

The main objective of this study was to develop microparticles with modified-release characteristics using a non-aqueous ESE method with a non-conventional stabilizer possessing a high HLB value. For this purpose, a hydrophilic API (paracetamol) was loaded in a biodegradable, thermo-responsive polymer – HPC.

Materials and methods

Materials

The API N-(4-hydroxyphenyl) acetamide (acetaminophen or paracetamol) was sourced from Zhejiang Kangle Pharmaceutical Co., Ltd. (China). Two types of HPC polymers (M_w = 80 kDa, η = 300–600 mPa s as per USP <912>, M_w = 95 kDa, η = 75–150 mPa s as per USP <912>) were obtained from Ashland (USA). The surfactant polyoxyethylene (80) sorbitan monooleate (M_w = 1308 Da) was obtained from Sigma Aldrich (Germany). Liquid paraffin, *n*-hexane, acetone, sodium hydroxide, and potassium dihydrogen were purchased from Alkaloid AD Skopje (North Macedonia). Methanol was purchased from Merck & Co. (Germany). Sodium hydroxide, potassium dihydrogen phosphate, and methanol were of analytical grade. Marketed paracetamol tablets with conventional and modified-release were purchased from drug stores.

Methods

Preparation of microparticles

The microparticles were prepared using an O_1/O_2 emulsion/solvent evaporation method. A schematic representation of the preparation process is shown in Fig. 1. This technique is appropriately classified as an oil-in-oil (O/O) system based on microencapsulation terminology, where the organic solvent containing the polymeric solution is considered as oil. The insolubility of both the drug and polymers in liquid paraffin makes it an ideal external phase for the emulsification process.

Firstly, paracetamol was dissolved in acetone at concentrations ranging of 1:13, 1:26, 1:39, and 1:52 (*w*/*v* %) using a magnetic stirrer set to 200 rpm to prepare the drug solution. The volume of acetone was adjusted empirically to achieve complete polymer solvation. The polymer was gradually added to the drug solution under continuous stirring to prevent lump formation. The API-to-polymer ratio was maintained between 1:1 and 1:4 (*w*/*w* %). Two types of HPC polymers were used in 1:1 ratio (*w*/*w* %) with different viscosities to achieve an optimal viscosity range for extrusion of the final API-polymer solution. The viscosity values of the HPC were 454 and 97 mPa s, respectively. During polymer solvation, the beaker was covered with parafilm to minimize acetone evaporation. The drug-polymer dispersion (O_1) was stirred using a magnetic stirrer at ambient temperature, with the stirring speed gradually reduced from 1000 to 150 rpm as the polymer dispersion transitioned to a more viscous and transparent state, yielding a drug-polymer solution. The solvation time was around 45 minutes.

The oil phase (O_2) was prepared by mixing 1 g of Tween 80 with 100 mL of liquid paraffin using a four-pitched blade mixer. A single emulsifier was employed to minimize interfacial tension and prevent droplet aggregation during emulsification and solvent evaporation. The ratio between internal phase (IP) and continuous phase (CP) ranged from 0.13 to 0.52.

The obtained organic API-polymer solution (O_1) was then slowly extruded dropwise through an immersed 23G (0.6 x 25 mm) needle into the oil phase (O_2). The resulting non-aqueous emulsion was stirred for at least four hours at ambient temperature to allow evaporation of the acetone and formation of microparticles. The end point of mixing was identified visually by the formation of solid, hard microparticles.

After two hours of mixing and acetone evaporation, approximately 15 mL *n*-hexane was added to the emulsion to facilitate hardening of the microparticles and their easier separation from the oil phase. Stirring continued throughout the evaporation process until complete solidification of the microparticles was achieved.

Once hardened, the microparticles were allowed to settle by gravity in the liquid paraffin. The continuous phase was decanted, and small portions (approximately 10 mL) of *n*-hexane were added several times to remove oil residues (liquid paraffin) and recover the microparticles from the beaker. They were transferred for vacuum filtration and were simultaneously rinsed of oil residues with *n*-hexane. The collected microparticles were air-dried for 24 h at ambient temperature (23±2 °C, RH ≤ 40 %) and stored in amber glass bottles containing silica gel until further use.

Characterization

ATR-IR spectroscopy

FT-IR spectra were recorded in the region 4000–550 cm^{-1}, using an ATR module with ZnSe crystal and low-pressure clamp, on Varian 660 FT-IR spectrometer, Varian Inc. All spectra were averaged from 16 scans per spectrum and the resolution was set to 4 cm^{-1}.

Morphology of microparticles

Particle morphology of the samples was analyzed using Zeiss Axioscope 5 microscope with Zeiss Axiocam 208 color camera using reflected light source, at magnification of 5x.

Particle size analysis

The volume distribution of microparticles was measured by laser diffraction using a Malvern Mastersizer 3000 equipped with a Hydro MV unit. Two light sources were utilized, a red He–Ne laser at 630 nm, and a blue LED at 470 nm. Optical properties for the particles were set at 1.520 refractive index and 0.100 absorption index. Liquid paraffin was used as a dispersant with the cell's stirrer speed set at 2200 rpm. Using light stirring, the samples were evenly distributed in liquid paraffin, as to avoid particle agglomeration.

Ultra-violet spectrometry

UV-vis spectrometry was used for quantitative analysis of encapsulation efficiency and drug release. The spectra were recorded with a UV-Vis spectrophotometer (Pharos 600, Merck) in the range 200–400 nm using a 10 mm quartz cell. The drug content was determined from the absorbances obtained at 243 nm.

Differential Scanning calorimetry

Weighed samples of 2–5 mg (measured using a Sartorius CPA225D-0CE balance) were scanned in aluminum pans with a perforated lids, at a speed of 10 K min^{-1}, from room temperature to 200 °C. All the samples were analyzed in dry nitrogen atmosphere using a Netzsch DSC 204F1 Phoenix instrument.

Determination of encapsulation efficiency of paracetamol

Encapsulation efficiency of microparticles was determined as previously reported[23]. All measurements were performed in triplicate. The encapsulation efficiency and encapsulated drug were calculated using Equations (1) and (2), respectively:

$$\text{Encapsulation efficiency [\%]} = W_1/W_2 \quad (1)$$

$$\text{Encapsulated API [\%]} = W_1/W_3 \quad (2)$$

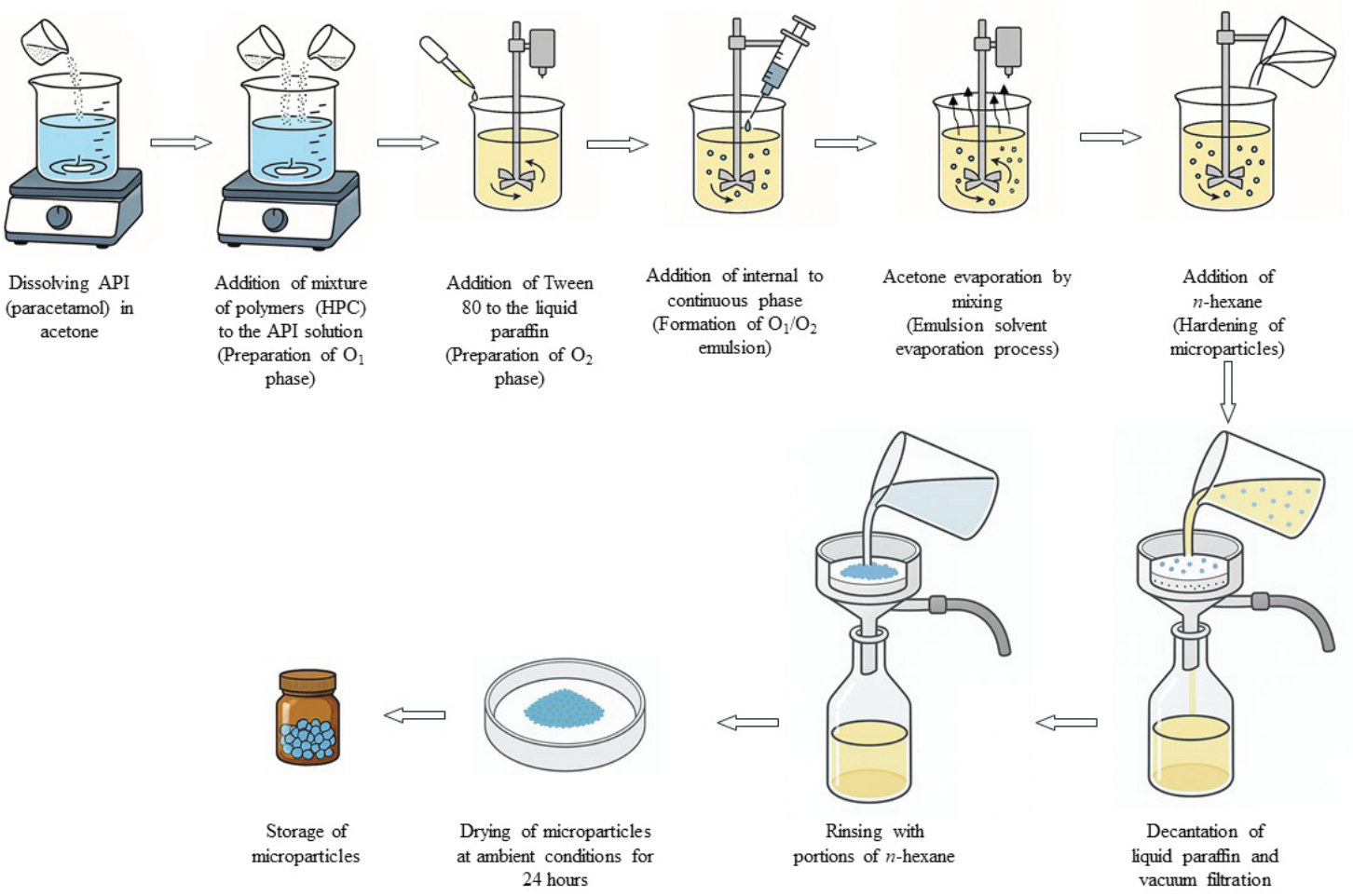

Fig. 1 – *Schematic representation of O_1/O_2 emulsion/solvent evaporation process for preparation of paracetamol microparticles*

where W_1 is the experimentally determined mass of API in the analyte [mg], W_2 is the theoretically determined mass of API in the analyte [mg], and W_3 is the mass of the sample in the trial [mg].

In vitro drug release study

The *in vitro* drug release from the microparticles was carried out as previously described[23]. The dissolution medium was phosphate buffer pH 6.8 (simulated duodenal medium and prepared as described in Ph.Eur. 5.17.1.). Microparticles (50 mg) were suspended in 250 mL, and one tablet was placed in 900 mL dissolution medium. Samples of the dissolution medium 2 mL (microparticles testing) and 5 mL (drug products testing) were withdrawn at different time points up to four hours fresh medium. Quantification was performed as described in the *Ultra-violet spectrometry* section.

Mathematical modelling of in vitro release

To evaluate the mechanisms of paracetamol release from the HPC-based microparticles and commercial drug product, model-dependent mathematical approaches (Table 1) were used. The obtained *in vitro* drug release was fitted to zero-order, first-order, Higuchi, Weibull, Korsmeyer-Peppas, and Hixson-Crowell models in Excel (Microsoft, Washington, USA). Based on the highest value for the coefficient of determination (R^2), the best fit model was considered.

Statistical evaluation

One-way analysis of variance (ANOVA) and Pearson's coefficient were carried out for comparison of results using Excel (Microsoft, Washington, USA). Differences were considered statistically significant at the level of α<0.05.

Results

Influence of formulation parameters on microsphere morphology and particle size

The microparticles appeared spherical, pseudo-spherical, and in some cases particle agglomeration was observed (Fig. 2). From the microphotograph, particle agglomeration was visible, and microparticles

Table 1 – *Mathematical models used to describe paracetamol release mechanisms*

Model	Equation	Parameters
Zero-order	$Q_t = Q_0 + k_0 \cdot t$	Q_t is the amount of dissolved drug in time t, Q_0 is the initial drug amount in the solution, k_0 is the zero-order constant
First-order	$\log Q_t = \log Q_0 + \frac{k_1 \cdot t}{2.303}$	Q_t is the amount of dissolved drug in time t, Q_0 is the initial drug amount in the solution, k_1 is the first-order constant
Higuchi	$Q_t = k_H \sqrt{t}$	Q_t is the amount of dissolved drug in time t, k_H is the Higuchi constant
Hixson-Crowell	$\sqrt[3]{W_0} = \sqrt[3]{W_i} + k_{HC} \cdot t$	W_0 is the amount of drug in pharmaceutical dosage form, W_i is the remaining amount of drug in the dosage form at time t, k_{HC} is proportionally constant
Korsmeyer-Peppas	$\frac{Q_t}{Q_\infty} = k \cdot t^n + b$	Q_t/Q_∞ fraction of released drug at time t, k is a release rate constant, n is the release exponent, b is burst effect
Weibull function	$\frac{Q_t}{Q_\infty} = 1 - \exp^{\frac{-(t-T_i)^\beta}{\alpha}}$	Q_t/Q_∞ fraction of the drug in solution as a function of time t, T_i is lag time measured as a result of the dissolution process, α is time scale, β describes the shape curve of dissolution profile

with different particle sizes among all trials were evident. The most spherical morphology was exhibited by T-4, with the highest polymer content.

The mean particle size (D[4,3]) ranged from 803 to 167 μm (Table 2), and the polymer content influenced the size variation.

Although a direct proportional relationship between particle size and polymer content was initially anticipated, the observed decrease in particle size may be attributed to the formation of a more efficient API–polymer matrix. An observation by Lee *et al.*[25] suggests that a higher amount of polymer can rapidly adsorb onto emerging drug aggregates, effectively limiting uncontrolled growth and coalescence, leading to a more controlled, uniform, and potentially smaller particle size distribution.

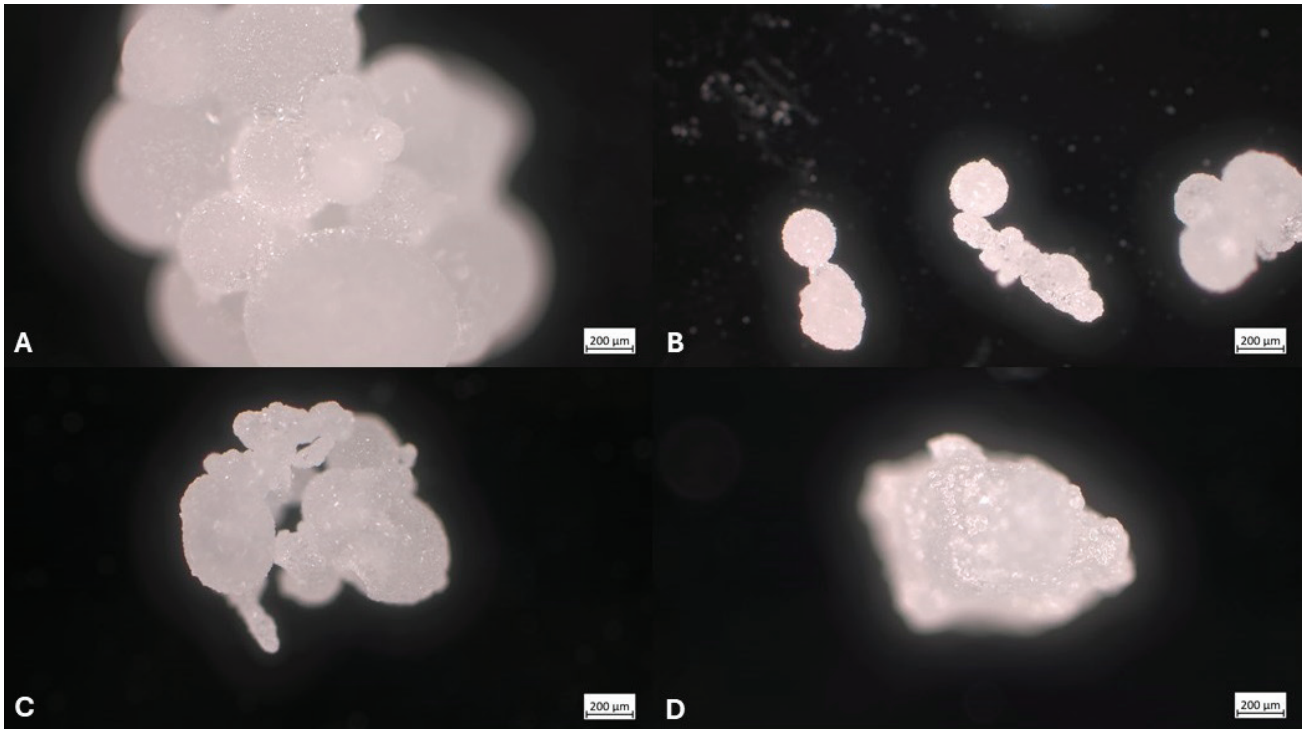

Fig. 2 – *Optical micrographs of paracetamol microparticles with modified release. T-4 with API:polymer ratio=1:4 (A), T-3 with API:polymer ratio=1:3 (B), T-2 with API:polymer ratio=1:2 (C), T-1 with API:polymer ratio=1:1 (D).*

Table 2 – *Results of particle size distribution*

	T-1	T-2	T-3	T-4
$D_{[4,3]}$ [μm]	803	666	562	197
Span	1.042	1.305	1.021	1.190

Drug-excipients interaction studies

FTIR was used to measure the IR spectrum (Fig. 3) of the API, HPC, and the laboratory trials to evaluate any possible interactions.

The IR spectrum of the API illustrates the characteristic bands of phenyl alcohol and the C=O vibrations of the amide group at 3321 and 1651 cm^{-1}, respectively. In addition, skeletal vibrations of C=C of the benzene and N–H (amide) can be discerned at 1609 and 1561 cm^{-1}, respectively[26]. A new band is noticed at 1736 cm^{-1} (C=O stretch), which is attributed to residues of the surfactant in the microparticles. The observed bands at 3411 cm^{-1} and 1644 cm^{-1} in the HPC IR spectrum are attributed to the adsorbed water which has significantly lower presence in the spectra of the microparticles. A gradient increase (T-4>T-3>T-2>T-1) in the intensity of the characteristic bands of paracetamol at: 3322, 1651, and 1560 cm^{-1} (phenol alcohol, carbonyl group from amide bond and amide group, respectively) in the IR spectra of trials is observed.

Differential scanning calorimetry

DSC analysis of pure paracetamol revealed a sharp endothermic melting peak at 171 °C (ΔH = 213.7 J g^{-1}), consistent with previously reported literature values[27]. The high molecular weight polymer exhibited a broad endothermic evaporation peak at approximately 68 °C, attributed to adsorbed moisture, and occurring at a lower temperature than that of the low molecular weight polymer.

The DSC thermogram of the microparticles (Fig. 4) displayed two broad endothermic transitions of reduced intensity. The first, observed between 66–85 °C, corresponds to the HPC polymer, while the second, occurring between 131–146 °C, is associated with the melting of paracetamol. The microparticles demonstrated thermal stability up to 200 °C.

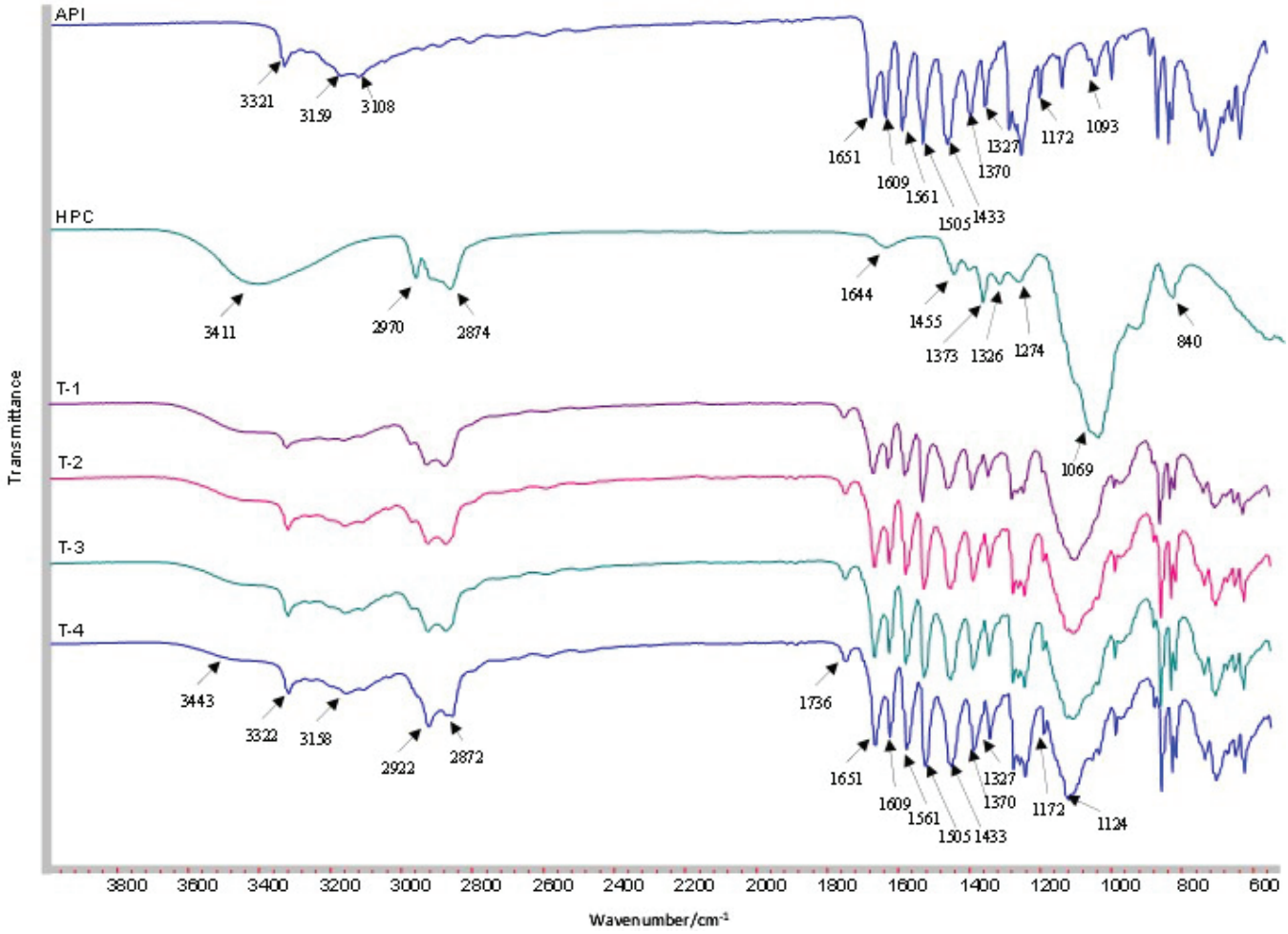

Fig. 3 – *FT-IR spectra of API, HPC, and laboratory trials*

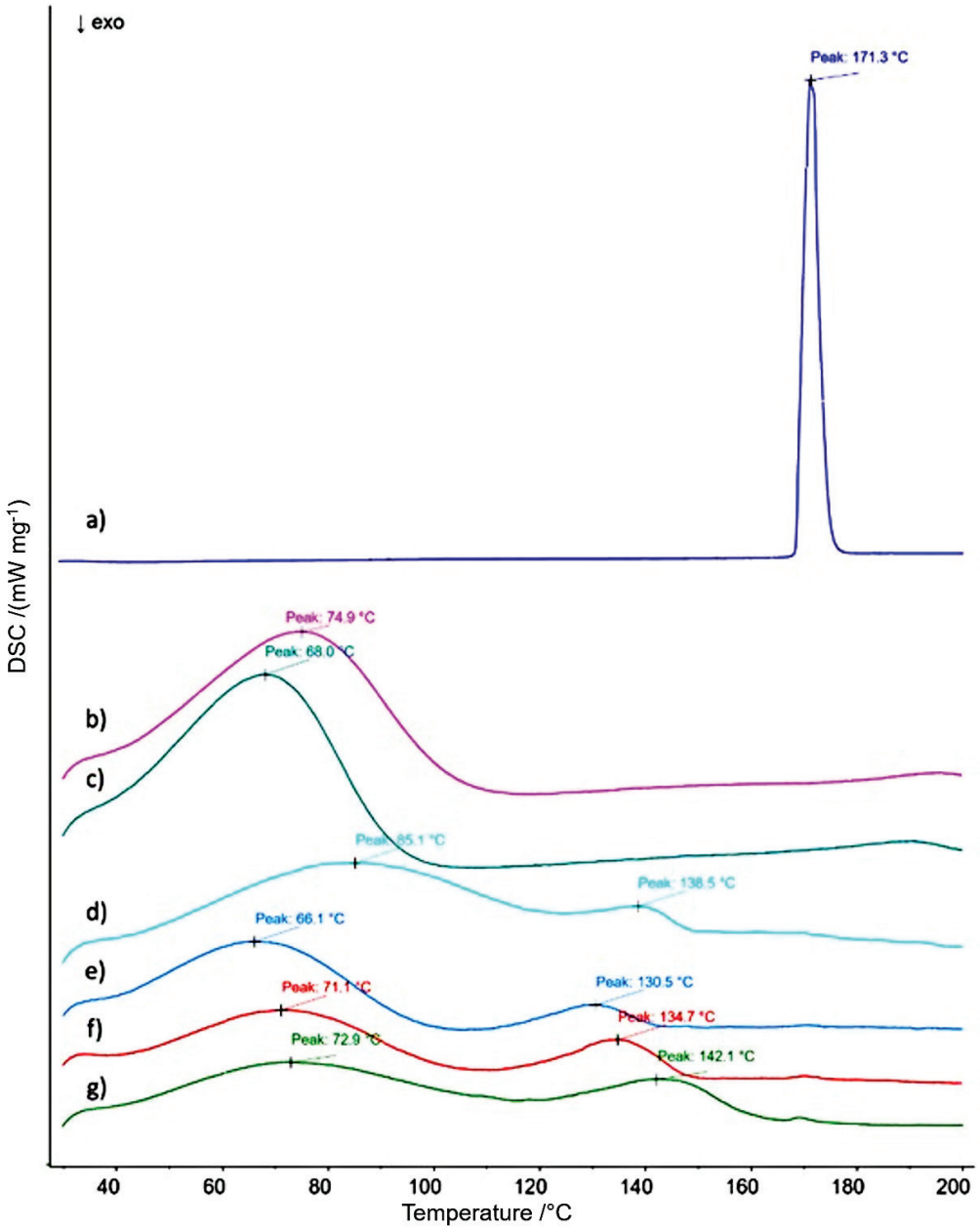

Fig. 4 – *DSC thermogram of a) paracetamol API; b) HPC with lower M_w; c) HPC with higher M_w; d) T-4; e) T-3; f) T-2; g) T-1*

The absence of a sharp characteristic endothermic melting peak of paracetamol in the thermograms of the microparticles indicates that encapsulation of the API in the polymer matrix has been achieved[29]. A higher polymer content in the investigated microparticles correlates with a lower melting temperature compared to a lower polymer content, leading to better possible solubilization and amorphization[30] of the API.

Influence of formulation parameters on encapsulation efficiency

Encapsulation efficiency (Table 3) of the trials was determined using the calibration curve method ($y = 0.01332x–0.0006$; $R^2 = 0.9992$). The fitting criteria for the calibration curve were compliant with the Guideline ICH Q2 (R2), *i.e.*, $R^2 \geq 0.99$. For that purpose, a series of standard solutions of paracetamol in the concentration range of 0.0003 – 0.0133 mg mL^{-1} from a stock solution (c = 1.62 mg mL^{-1}) in solvent methanol and water (45:55, *v*/*v*) were prepared and measured at λ_{max} = 243 nm on a UV-Vis spectrophotometer. The percentage of encapsulated paracetamol with modified release ranged from 52.20 % to 73.15 %, whereas the drug loading varied from 14.05 % to 23.70 %.

Statistical analysis using ANOVA and Pearson's correlation coefficient supports these observations. Encapsulation efficiency significantly increased with

Table 3 – *Results of encapsulation efficiency and drug loading*

Trial code	API: Polymer content ratio [*w*/*w*]	IP/CP [*v*/*v*]	Encapsulation efficiency [%]	Drug loading [%]	Theoretical drug content [*w*/*w* %]	Amount of entrapped drug [*w*/*w* %]
T-4	1:4	0.52	73.15	14.05	20.00	14.63
T-3	1:3	0.39	62.30	15.55	25.00	15.58
T-2	1:2	0.26	60.00	18.70	33.33	20.00
T-1	1:1	0.13	52.20	23.70	50.00	26.10

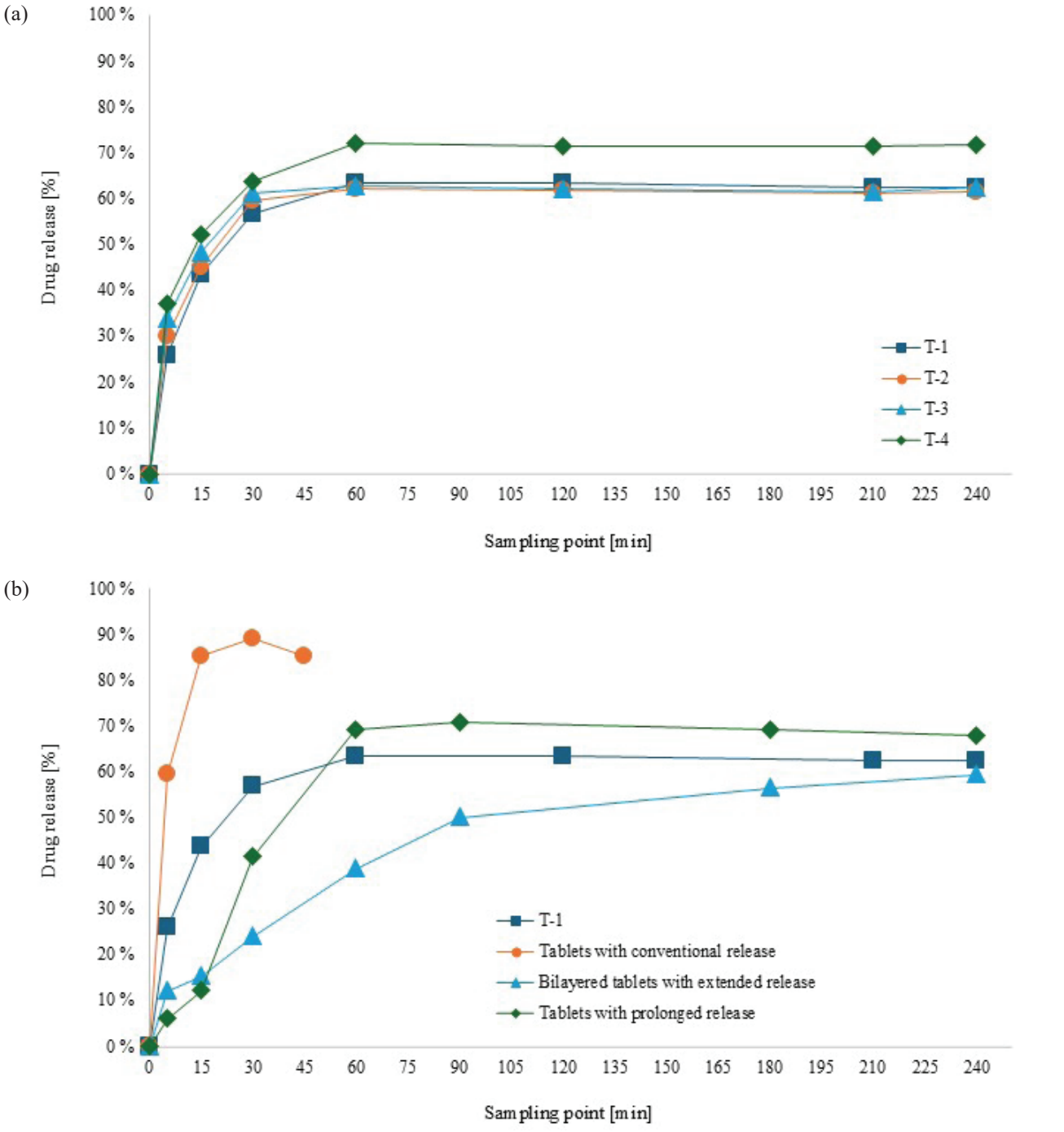

Fig. 5 – *Dissolution profiles of paracetamol trials (a), and paracetamol trial vs. commercial drug products (b)*

Table 4 – *Release kinetics of formulation trials*

Model	Parameter	T-1	T-2	T-3	T-4
Zero order	D	0.001	0.001	0.001	0.001
	R^2	0.419	0.373	0.357	0.469
First order	K	$-4\cdot10^{-6}$	$-3\cdot10^{-6}$	$-3\cdot10^{-6}$	$-4\cdot10^{-6}$
	R^2	0.419	0.373	0.357	0.469
Higuchi	K_H	0.021	0.018	0.015	0.021
	R^2	0.594	0.541	0.521	0.643
Hixson-Crowell	K_{HC}	$-2\cdot10^{-5}$	-10^{-5}	-10^{-5}	-10^{-5}
	R^2	0.419	0.373	0.358	0.469
Weibull	β	0.206	0.166	0.139	0.159
	R^2	0.778	0.748	0.734	0.826
Korsmeyer-Peppas 60 %	n	0.44	0.38	0.33	0.30
	R^2	0.996	0.999	0.999	0.999

rising polymer content ($p<0.001$, $r = 0.923$) and with a higher IP/CP ratio (internal phase to continuous phase ratio) of the emulsion ($p<0.001$, $r = 0.972$). The interaction of polymer content and IP/CP ratio also significantly influenced drug loading ($p<0.001$, $r = 0.503$) and ($p<0.001$, $r = 0.685$), respectively.

Influence of formulation parameters on *in vitro* drug release

The dissolution of the trials and commercial drug products was determined using the calibration curve method ($y = 0.0144x–0.0001$; $R^2 = 0.9999$). The fitting-criteria for the calibration curve were compliant with the Guideline ICH Q2 (R2), *i.e.* $R^2 \geq 0.99$. For that purpose, a series of standard solutions of paracetamol in the concentration range of 0.0003 – 0.0133 mg mL^{-1} diluted from a stock solution ($c = 1.622$ mg mL^{-1}) in phosphate buffer pH 6.8 were prepared and measured at $\lambda_{max} = 243$ nm on a UV-Vis spectrophotometer. The *in vitro* dissolution profiles of lab trials and commercial drug products in medium pH 6.8 are shown in Fig. 5, (a) and (b), respectively.

In the trial T-1 with a 1:1 ratio (API:polymer), lower drug release over time can be observed compared to trial T-4 (1:4 ratio). The drug released percentage correlates with the encapsulation efficiency, as summarized in Table 3.

In addition, the trial with the slowest dissolution profile (T-1) was compared with commercially available drug products: one with conventional-release, one with prolonged-release, and one with extended-release (Fig. 5(b)). From the presented dissolution profiles, it can be observed that trial T-1 exhibits prolonged release compared to tablets with conventional release mechanism. Compared to marketed drug products with extended- or prolonged-release, trial T-1 shows a slightly faster drug release profile. These observations can serve as a potential research field in the process of formulation development and optimization.

Pharmacokinetic study

The coefficients from the pharmacokinetic study are summarized in Table 4.

As shown in Table 4 and Fig. 6, the Weibull model provided the best fit across all four trials. The β-coefficients ($\beta < 1$) indicate a diffusion-controlled release mechanism. This interpretation is further supported by the Korsmeyer–Peppas model and $Q\sqrt{t}$ dependence by Higuchi model, where the calculated release exponent values ($n < 0.43$) fall below the threshold typically associated with Fickian diffusion in spherical systems.

The n-value for T-1 is borderline ($n = 0.44$) but is lower than 0.5, indicating an anomalous transport (polymer relaxation, erosion, and diffusion) according to the theoretical thresholds. Yet, in correlation with the obtained kinetic data and dissolution profiles, a diffusion-controlled release may be implied. A reverse proportional dependence is evident among the n-values and polymer content in the trials, *i.e.,* more diffusion-controlled release mechanisms are present in formulations with higher polymer content. This phenomenon can be attributed to a denser, more uniform matrix formed by higher polymer content, thus the API molecules face greater resistance to diffuse through the polymer matrix.

Table 5 – *Release kinetics of commercial drug products*

Model	Parameter	ER	CR	PR
Zero order	D	0.002	0.005	0.002
	R^2	0.829	0.500	0.509
First order	K	$-9\cdot10^{-6}$	$-2\cdot10^{-5}$	-10^{-5}
	R^2	0.829	0.500	0.506
Higuchi	K_H	0.039	0.057	0.049
	R^2	0.939	0.641	0.691
Hixson-Crowell	K_{HC}	$-3\cdot10^{-5}$	$-9\cdot10^{-5}$	$-4\cdot10^{-5}$
	R^2	0.829	0.500	0.506
Weibull	β	0.461	0.174	0.68
	R^2	0.962	0.782	0.845
Korsmeyer-Peppas 60 %	n	0.46	0.239	1.06
	R^2	0.962	0.918	0.925

Legend: ER – extended release, CR – conventional release, PR-prolonged release

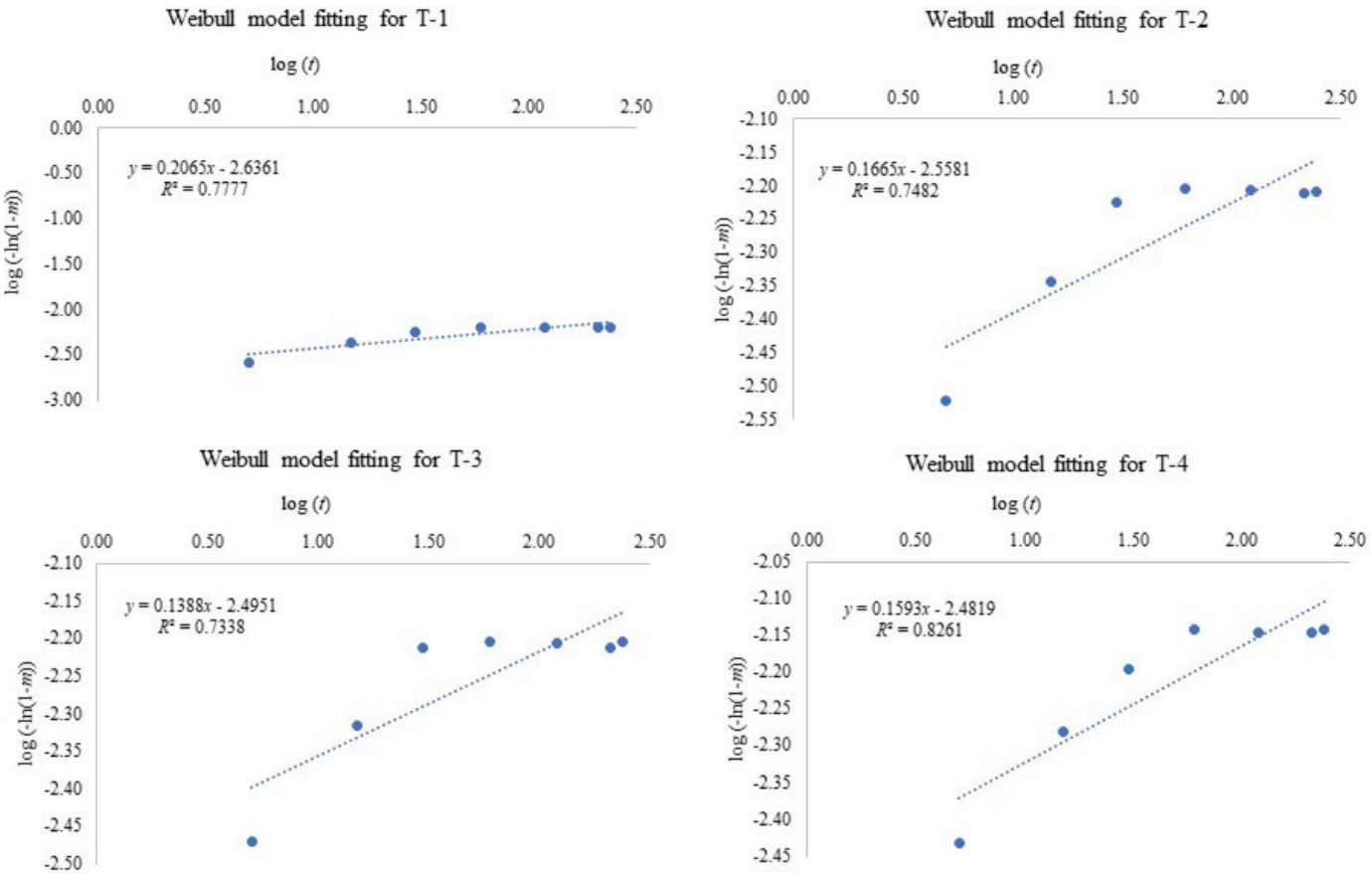

Fig. 6 – *Weibull model fitting curves for drug release profiles across trials*

The *n*-values for Korsmayer-Peppas model observed in the kinetics for commercial drug products (Table 5) correspond to anomalous transport ($n = 0.46$, extended-release tablets) and super II case transport ($n = 1.06$, prolonged-release tablets). Unlike the release mechanism observed in the trials, which was governed by a combination of polymer relaxation and diffusion, the prolonged-release tablets exhibited a release mechanism predominantly driven by polymer matrix swelling and drug release facilitated by matrix expansion, rather than diffusion. Fig. 7 displays the Weibull model fitting curves for tested commercial drug products.

Discussion

Microscopic analysis revealed evident particle agglomeration and notable variation in microparticle size across all trials. This phenomenon is likely attributable to the use of a high-HLB, hydrophilic surfactant-Tween 80, which may not be optimal for stabilizing oil-in-oil (O/O) emulsions. In such systems, insufficient interfacial adsorption can lead to droplet coalescence and poor dispersion stability[37]. To mitigate this, future work will explore HLB blending strategies[38], such as combining Tween 80 with a low-HLB surfactant like Span 80, to fine-tune interfacial tension and enhance emulsion stability. Furthermore, during the preparation process, it was observed that increasing the internal phase volume while maintaining a constant continuous phase volume led to a progressive increase in particle agglomeration, because of the reduced space for droplets to move during mixing phase, causing them to collide more frequently. This also extends solvent evaporation time because the increased particle density requires more energy and time for the solvent to escape from the larger mass of droplets. Thereafter, it may be observed that IP/CP ratio plays a critical role in emulsion stability and droplet dispersion. In the research it has been observed that the phase volume/emulsifier HLB ratio results in an appropriate optimum stability[39], that further corroborates our hypothesis. Accordingly, we propose the IP/CP ratio as a second dependent variable for optimization. Based on the observed trends, further adjustment of the evaporation time may be warranted to accommodate changes in phase ratio and mitigate agglomeration, thereby improving particle uniformity and process reproducibility. The proposed approaches are expected to reduce agglomeration and improve particle uniformity.

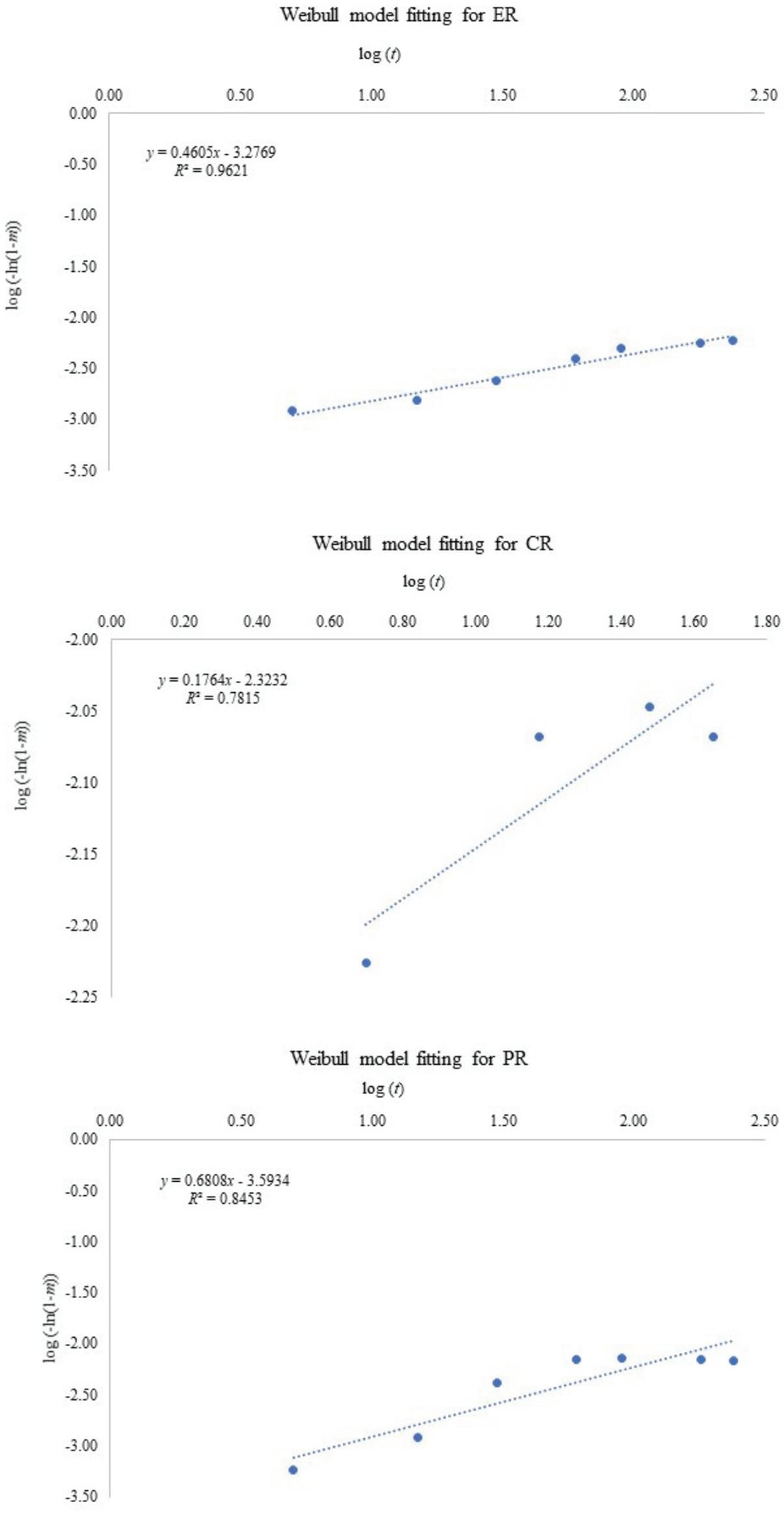

Fig. 7 – *Weibull model fitting curves for drug release profiles across commercial drug products*

Based on the results (Table 1), the particle size is reduced by increasing the polymer content (T-4<T-3<T-2<T-1). This observation agrees with the inverse dependence established between IP/CP ratio and average particle size in an O/O ESE system[20]. Nethaji *et al.*[24] reported a significant increase in particle size with increasing polymer content, attributing this trend to elevated droplet viscosity, which led to the formation of larger droplets and consequently larger microspheres. In contrast, viscosity was not the primary focus of the present study; instead, the API-to-polymer ratio was systematically varied, while the organic solvent-to-polymer ratio was maintained constant at 13:1 (*v*:*w*) across all trials.

The observed differences in particle size may be more closely associated with the IP/CP ratio, which ranged from 0.13 to 0.52. This variation may have hindered complete evaporation of the organic solvent, potentially resulting in residual acetone entrapped within the microparticles. Such entrapment could further influence the internal morphological porosity, affecting the structural integrity and performance characteristics of the microparticles.

From the IR spectra of the laboratory trials, no significant band shifts with respect to paracetamol could be observed, thus confirming the compatibility of the excipients and API. The trend in gradient increase (T-4>T-3>T-2>T-1) correlates with the encapsulation efficiency data, thus confirming the drug encapsulation in the polymer matrix. The developed drug delivery systems demonstrated satisfactory encapsulation efficiency, confirming the successful formulation strategy. Among the tested formulations, Trial 4 exhibited the highest encapsulation efficiency, whereas Trial 1 showed the lowest. Conversely, Trial 1 achieved the highest drug loading, while Trial 4 presented the lowest. These findings suggest a direct proportional relationship between polymer content and encapsulation efficiency, which aligns with findings reported by Yang *et al.*[28], who observed increased encapsulation efficiency of aspirin with higher ethyl cellulose content.

In this study, the Weibull equitation was able to fit all data sets adequately to the R^2. The model had the best fit in any of the sets, even though it is an empirical model and is expected to have poor predictive power[32], which was not the case in the present research. Weibull has two geometric main parameters, scale factor α (the intercept, expressed as $\ln(\alpha)$), and shape factor of the release curve β (the slope). A tendency towards a parabolic shape could be observed from the dissolution profiles, as all curves are compliant with $\beta<1$ [32]. In the literature[33], the relationship between the Weibull β-parameter and Korsmeyer-Peppas parameter n have been proposed and analyzed. Doing this analysis with n and β parameters in the present study, it can be concluded that Fickian diffusion is the main drug release mechanism from the HPC microparticles, whereas the commercial drug products with prolonged release are complex. Similar findings have been obtained in PLGA nanoparticles[33,34].

To complement the Weibull empirical model, further analysis with Higuchi's model was performed. Tables 5 and 6 display that Higuchi model showing subsequent best fit model following Weibull. All four formulations and commercial drug products are $Q\sqrt{t}$ (Higuchi's model) compliant, thus confirming that a matrix-structure with sustained diffusion-controlled release is obtained. The results are consistent with other relevant research studies[35,36].

Conclusion

The O_1/O_2 ESE method, a relatively uncommon approach, was successfully employed to formulate paracetamol-loaded microparticles with modified-release properties. The thermo-responsive biopolymer HPC served as the drug carrier, while Tween 80 was utilized to stabilize the oil-in-oil emulsion system. Although Tween 80 is conventionally used in aqueous emulsions, the findings from this study demonstrate its efficacy in stabilizing non-aqueous emulsions containing a hydrophilic polymer, specifically within the ESE framework. In this context, Tween 80 functions as an interfacial stabilizer between acetone (dispersed phase) and liquid paraffin (continuous phase).

Among the formulations, Trial T-4, which contained the highest polymer concentration, exhibited the most spherical particle morphology. A direct correlation was observed between polymer content and both encapsulation efficiency and drug release rate, while solid-state characterization confirmed the absence of drug–polymer interactions. Conversely, a reverse correlation was noted between polymer content and both mean particle size and drug loading capacity. While its drug loading was relatively low, the formulation's performance supports its suitability for preliminary development, with future optimization focused on enhancing drug payload without compromising release characteristics or patient compliance. Modified drug release was achieved. Based on the obtained data, a subsequent experimental phase will be conducted using a D-optimal design, incorporating polymer content as the most influential formulation variable alongside key process parameters such as stirring rate and evaporation time. Additionally, visual observations during the technological process suggest that the

continuous phase plays a critical role in both particle agglomeration and the evaporation rate of the organic solvent from the internal phase. Accordingly, it may be considered a dependent variable in the next investigational phase. It is encouraged that future studies incorporate advanced analytical methods for quantifying Tween 80 residues to ensure compliance with pediatric exposure limits and strengthen the formulation's safety profile. Future work will include mechanistic modeling to deepen the understanding of drug release dynamics in the optimized formulation identified through the current QbD-driven design, and will extend to *in vitro – in vivo* correlations to support its translational and biopharmaceutical relevance.

Abbreviations

ΔH – change in enthalpy (heat absorbed or released), J or in DSC J g^{-1}
ANOVA – analysis of variance
API – active pharmaceutical ingredient
ATR – attenuated total reflectance (FTIR sampling technique)
c – concentration, mg mL^{-1}
COX – cyclooxygenase
CP – continuous phase
DSC – Differential Scanning Calorimetry
EMA – European Medicines Agency
ESE – emulsion solvent evaporation
EU – European Union
FDA – Food and Drug Administration (U.S.)
FTIR – Fourier-transform infrared spectroscopy
HLB – hydrophile–lipophile balance
HPC – hydroxypropyl cellulose
HPMC – hydroxypropyl methylcellulose
ICH – International Council for Harmonisation of Technical Requirements for Pharmaceuticals for Human Use
IP – internal phase
LCST – lower critical solution temperature
MDD – maximum daily dose
M_w – weight-average molar mass, g mol^{-1}
O/O – oil-in-oil (emulsion type)
OTC – over-the-counter (medication)
Ph.Eur. – European Pharmacopoeia
PLGA – poly(lactic-co-glycolic acid)
Q – quantity, mg
R^2 – coefficient of determination
RH – relative humidity
TGA – Therapeutic Goods Administrations (Australia)
USA – United States of America
UV-Vis – ultraviolet-visible
W – weight, mg
W/O – water-in-oil (emulsion type)
η – viscosity, mPa s

References

1. *Flynn, R., Hedenmalm, K.,* Prescribing of paracetamol in patients with chronic renal failure, EMA, Amsterdam, 2019.
2. *Tripathy, K. D.,* Essential of Medical Pharmacology (5th ed.). Jaypee Brothers Medical Publishers (P) Ltd, New Delhi, 2003.
3. URL: https://www.tga.gov.au/news/news/recommended-paracetamol-doses (16.02.2025)
4. URL: https://www.tga.gov.au/sites/default/files/2022-09/paracetamol_report_final.pdf (16.02.2025)
5. URL: https://www.ema.europa.eu/en/medicines/human/referrals/paracetamol-modified-release (16.02.2025)
6. *Yelland, M. J., Nikles, C. J., McNairn, N., Del Mar, C. B., Schluter, P. J., Brown, R. M.,* Celecoxib compared with sustained-release paracetamol for osteoarthritis: A series of n-of-1 trials, Rheumatol. Oxford, England, 2007, pp. 135–140.
doi: https://doi.org/10.1093/rheumatology/kel195
7. *Beena Unni, A., Muringayil Joseph, T.*, Enhancing polymer sustainability: Eco-conscious strategies, Polym. J. **16** (2024) 1769.
doi: https://doi.org/10.3390/polym16131769
8. *Abdul Wasay, S., Umer Jan, S., Akhtar, M., Noreen, S., Gul, R.,* Developed meloxicam loaded microparticles for colon targeted delivery: Statistical optimization, physicochemical characterization, and *in-vivo* toxicity study, PLOS ONE **17** (2022) e0267306.
doi: https://doi.org/10.1371/journal.pone.0267306
9. *Arefin, P., Hasan, I., Reza, M. S.*, Design, characterization and *in vitro* evaluation of HPMC K100 M CR loaded Fexofenadine HCl microspheres, SpringerPlus **5** (2016) 691.
doi: https://doi.org/10.1186/s40064-016-2322-2
10. *Curcio, C., Greco, A. S., Rizzo, S., Saitta, L., Musumeci, T., Ruozi, B., Pignatello, R.,* Development, optimization and characterization of Eudraguard®-based microparticles for colon delivery, Pharmaceuticals **13** (2020) 131.
doi: https://doi.org/10.3390/ph13060131
11. *Wei, S., Ma, Y., Luo, J., He, X., Yue, P., Guan, Z., Yang, M.,* Hydroxypropyl cellulose as matrix carrier for novel cage-like microparticles prepared by spray-freeze-drying technology, Carbohydr. Polym. **157** (2017) 953.
doi: https://doi.org/10.1016/j.carbpol.2016.10.043
12. *Sarode, A. L., Malekar, S. A., Cote, C., Worthen, D. R.*, Hydroxypropyl cellulose stabilizes amorphous solid dispersions of the poorly water-soluble drug felodipine, Carbohydr. Polym. **112** (2014) 512.
doi: https://doi.org/10.1016/j.carbpol.2014.06.039
13. *Rashid, R., Kim, D. W., Din, F., Mustapha, O., Yousaf, A. M., Park, J. H., Kim, J. O., Yong, C. S., Choi, H.*, Effect of hydroxypropyl cellulose and Tween 80 on physicochemical properties and bioavailability of ezetimibe-loaded solid dispersion, Carbohydr. Polym. **130** (2015) 26.
doi: https://doi.org/10.1016/j.carbpol.2015.04.071
14. *Imeson, A.*, Cellulose derivates, in: Cash, M., Caputo, S. (Eds), Food Stabilizers, Thickeners and Gelling Agents, Wiley-Blackwell Publishing Ltd. Chichester, 2010, pp 95–113.

15. *Arca, H. C., Mosquera-Giraldo, L. I., Bi, V., Xu, D., Taylor, L. S., Edgar, K. J.,* Pharmaceutical applications of cellulose ethers and cellulose ether esters, Biomacromolecules **19** (2018) 2351. doi: https://doi.org/10.1021/acs.biomac.8b00517
16. Ph. Eur. Monograph 0337, Hydroxypropyl cellulose, European Pharmacopoeia, 11th Edition, Council of Europe, Strasbourg, 2025.
17. *Gosecki, M., Setälä, H., Virtanen, T., Ryan, A. J.*, A facile method to control the phase behavior of hydroxypropyl cellulose, Carbohydr. Polym. **251** (2021) 117015. doi: https://doi.org/10.1016/j.carbpol.2020.117015
18. *Joseph, B., Sagarika, V. K., Sabu, C., Kalarikkal, N., Thomas, S.*, Cellulose nanocomposites: Fabrication and biomedical applications, J. Bioresour. Bioprod. **5** (2020) 223. doi: https://doi.org/10.1016/j.jobab.2020.10.001
19. *Suitthimeathegorn, O., Turton, J. A., Mizuuchi, H., Florence, A. T.*, Intramuscular absorption and biodistribution of dexamethasone from non-aqueous emulsions in the rat, Int. J. Pharm. **331** (2007) 204. doi: https://doi.org/10.1016/j.ijpharm.2006.11.062
20. *Meng, F., Wang, S., Wang, Y., Liu, H., Huo, X., Ma, H., Ma, Z., Xiong, H.*, Microencapsulation of oxalic acid via oil-in-oil (O/O) emulsion solvent evaporation, Powder Technol. **320** (2017) 405. doi: https://doi.org/10.1016/j.powtec.2017.07.073
21. The HLB SYSTEM a time-saving guide to emulsifier selection, ICI Americas Inc., Delware, 1976.
22. *Poteshnova, M. V., Zadymova, N. M.*, Aqueous solutions of hydroxypropyl cellulose, Tween 80 and their binary mixtures: Colloid-chemical aspects, Colloid J. **79** (2017) 797. doi: https://doi.org/10.1134/S1061933X17060126
23. *Georgievska, T., Atkovska, K., Lisichkov, K.*, The influence of stirring rate in emulsion solvent evaporation method on biopharmaceutical properties of microparticles containing acetaminophen, Contributions, Sec. Nat. Math. Biotech. Sci., MASA **42** (2023) 45. doi: https://doi.org/10.20903/masa/nmbsci.2021.42.6
24. *Nethaji, R., Shahana, P., Binulal, C., Palanivelu, C. M., Surendiran, N. S., Ganesan, B.*, Formulation and evaluation of paracetamol loaded mucoadhesive microspheres, Int. J. Pharm. Pharmacol. **1** (2017) 106. doi: https://doi.org/10.31531/2581-3080.1000106
25. *Lee, K. H., Khan, F. N., Cosby, L., Yang, G., Winter, J. O.,* Polymer concentration maximizes encapsulation efficiency in electrohydrodynamic mixing nanoprecipitation, Front. Nanotechnol. **3** (2021) 719710. doi: https://doi.org/10.3389/fnano.2021.719710
26. *Zapata, F., Fernández, A. L., Ojeda, F. O., Quintanilla, G., Ruiz, C. G., Montalvo, G.*, Introducing ATR-FTIR spectroscopy through analysis of acetaminophen drugs: Practical lessons for interdisciplinary and progressive learning for undergraduate students, J. Chem. Educ. **98** (2021) 2675. doi: https://doi.org/10.1021/acs.jchemed.0c01231
27. Ph. Eur., Paracetamol, Monograph 0049, European Pharmacopoeia, 11th Edition, Council of Europe, Strasbourg, 2022.
28. *Yang, C. Y., Tsay, S. Y., Tsiang, R. C.,* An enhanced process for encapsulating aspirin in ethyl cellulose microcapsules by solvent evaporation in an O/W emulsion, J. Microencapsul. **17** (2000) 269. doi: https://doi.org/10.1080/026520400288256
29. *Chikukwa, M. T. R., Walker, R. B., Khamanga, S. M. M.,* Formulation and characterization of a combination captopril and hydrochlorothiazide microparticulate dosage form, Pharmaceutics **12** (2020) 712. doi: https://doi.org/10.3390/pharmaceutics12080712
30. *Luebbert, C., Huxoll, F., Sadowski, G.*, Amorphous-amorphous phase separation in API/polymer formulations, Molecules **22** (2017) 296. doi: https://doi.org/10.3390/molecules22020296
31. *Jahromi, L. P., Ghazali, M., Ashrafi, H., Azadi, A.,* A comparison of models for the analysis of the kinetics of drug release from PLGA-based nanoparticles, Heliyon **6** (2020) e03451. doi: https://doi.org/10.1016/j.heliyon.2020.e03451
32. *Kobryń, J., Sowa, S., Gasztych, M., Dryś, A., Musiał, W.,* Influence of hydrophilic polymers on the β factor in Weibull equation applied to the release kinetics of a biologically active complex of aesculus hippocastanum, Int. J. Polym. Sci. **2017** (2017) 3486384 doi: https://doi.org/10.1155/2017/3486384
33. *Heredia, N. S., Vizuete, K., Calero, M. F., Pazmiño, K. V., Pilaquinga, F., Kumar, B., Debut, A.,* Comparative statistical analysis of the release kinetics models for nanoprecipitated drug delivery systems based on poly(lactic-co-glycolic acid), PLoS ONE **17** (2022) e0264825. doi: https://doi.org/10.1371/journal.pone.0264825
34. *Papadopoulou, V., Kosmidis, K., Vlachou, M., Macheras, P.,* On the use of the Weibull function for the discernment of drug release mechanisms, Int. J. Pharm. **309** (2006) 44. doi: https://doi.org/10.1016/j.ijpharm.2005.10.044
35. *Jelvehgari, M., Montazam, S. H.,* Comparison of microencapsulation by emulsion-solvent extraction/evaporation technique using derivatives cellulose and acrylate-methacrylate copolymer as carriers, Jundishapur J. Nat. Pharm. Prod. **7** (2012) 144.
36. *Özdemir, N., Tilkan, M. G. Y.,* Investigation of the parameters affecting the release of flurbiprofen from chitosan microspheres, Braz. J. Pharm. Sci. **53** (04) (2017). doi: https://doi.org/10.1590/s2175-97902017000400242
37. *Cai, Z., Wei, Y., Shi, A., Zhong, J., Rao, P., Wang, Q., Zhang H.,* Correlation between interfacial layer properties and physical stability of food emulsions: Current trends, challenges, strategies, and further perspectives, Adv. Colloid Interface Sci. **313** (2023) 102863. doi: https://doi.org/10.1016/j.cis.2023.102863
38. *Mahdi, E. S., Sakeena, M., Abdulkarim, M., Abdullah, G., Abdul Sattar, M. Z., Noor, A. M.,* Effect of surfactant and surfactant blends on pseudoternary phase diagram behavior of newly synthesized palm kernel oil esters, Drug Des. Devel. Ther. **5** (2011) 311. doi: https://doi.org/10.2147/DDDT.S15698
39. *Sepulveda, E., Kildsig, D. O., Ghaly, E. S.,* Relationship between internal phase volume and emulsion stability: The cetyl alcohol/stearyl alcohol system, Pharm. Dev. Technol. **8** (2003) 263. doi: https://doi.org/10.1081/PDT-120022155